

# Detailed hydrodynamic instability structure at hydrogen/air detonation front using WCNS scheme

Ryohei Iida<sup>1</sup>, Makoto Asahara<sup>1</sup>, Nobuyuki Tsuboi<sup>2</sup>, Taku Nonomura<sup>3</sup>, A.Koichi Hayashi<sup>1</sup>

<sup>1</sup>Department of Mechanical Engineering, Aoyamag Gakuin University  
5-10-1 Fuchinobe, Chuo, Sagamihara, Kanagawa 252-5258 Japan

<sup>2</sup>Kyushu Institute of Technology  
1-1 Sensui, Tobata, Kitakyushu, Fukuoka, 804-8550 Japan

<sup>3</sup>JAXA/Institute of Space and Astronautical Science  
3-1-1 Yoshinodai, Chuo, Sagamihara, Kanagawa, 252-5210 Japan

Key words: WCNS, Detonation, Detonation front

## 1 Introduction

Two-dimensional detonation has been simulated since Taki and Fujiwara<sup>[1]</sup> started in 1978. Computers and numerical schemes have been improved dramatically since then. There are at least two approaches to improve detonation calculation besides chemical mechanism: one is scheme itself and another is time and space resolution.

As far as scheme, Godunov scheme, Harten Yee TVD scheme, HLLE scheme, AUSMDV scheme, WENO scheme have been used for detonation up to now. On the other hand small grid size has been applied to get a high resolution using AMR method (see Radulescu et al.<sup>[2]</sup>). They said the grid size must need at least  $10^4$  of a half reaction length. Comparing these two approaches, the approach by improving scheme instead of increasing number of grid points must be costless to get a reasonable hydrodynamic instability of detonation structure. Recent paper by Asahara et al.<sup>[3]</sup> presents the multi-dimensional numerical simulation of hydrogen detonation using an ASUMDV scheme<sup>[4]</sup>. To get the further detailed detonation structure, a dozen billions grid points are necessary to see such fine structure.

This paper presents a high resolution scheme that is able to ensure enough resolution with a small amount of grid points. A weighted compact nonlinear scheme<sup>[5-7]</sup> (WCNS), that enable to provide conserved values to AUSMDV, is introduced to calculate a detailed structure. However, the original WCNS fails to calculate detonation easily. Hence a robust WCNS, which is improved by Nonomura and Fujii<sup>[8]</sup>, is used instead to perform high resolved grid system simulation of detonation stability.

## 2 Governing equations

This paper deals with hydrogen-air compressible Euler equations with mass conservation, momentum conservation law, and energy conservation laws. Reactive gases consist of nine chemical species;  $H_2$ ,  $O_2$ ,  $O$ ,  $H$ ,  $OH$ ,  $HO_2$ ,  $H_2O_2$ ,  $H_2O$ ,  $N_2$ . For chemical reaction, Petersen and Hanson model<sup>[9]</sup> is applied with 18 elementary reactions.

### 3 Numerical method

To integrate compressible Euler equations, A strong stability preserving Runge-Kutta method<sup>[10]</sup> (SSPRK) is used for time integration, third order AUSMDV is used for the convective term. In interpolation of conservation quantity, WCNS is introduced into nonlinear interpolation of conservation quantity whose robust linear scheme is presented by Nonomura and Fujii. For comparing with newly introduced scheme, a third order MUSCL<sup>[11]</sup> scheme for nonlinear interpolation and central difference method for linear interpolation are used.

#### 3.1 Nonlinear interpolation

WCNS is the interpolation method combined with Compact and WENO scheme, which has advantages that its resolution is higher than the original WENO and its flux evaluations are used with AUSMDV.

The  $(2r-1)$ th-order WCNS calculates by following ways.

- I. Interpolate conservation quantity on each cell point to characteristic quantities with stencil.
- II. Construct polynomials of characteristic quantities for every substencil which number is  $r$ .
- III. Execute weighted average for characteristic quantities. Each weight for the polynomials increase as the polynomial gets smoothed.
- IV. Obtain conservation quantity by the right vector.

#### 3.2 Linear interpolation

Linear interpolation of the  $(2r-1)$ th-order ordinary WCNS is defined as

$$\mathbf{E}'_j = \frac{1}{\Delta x} \sum_{k=1}^{r-1} a_k (\tilde{\mathbf{E}}_{j+k/2} - \tilde{\mathbf{E}}_{j+k-1/2}) \quad (1)$$

Coefficient  $a_k$  is the known fixed number.

On the other hand, the linear interpolation suggested by Nonomura and Fujii is described as

$$\mathbf{E}'_j = \frac{1}{\Delta x} \sum_{k=1}^{r-1} b_k (\tilde{\mathbf{E}}_{j+k/2} - \tilde{\mathbf{E}}_{j-k/2}) \quad (2)$$

$$\tilde{\mathbf{E}}_{j+k/2} = \begin{cases} \tilde{\mathbf{E}}_{j+k/2} & (k = 2n-1) \\ \tilde{\mathbf{E}}_{j+k/2} & (k = 2n) \end{cases} \quad (3)$$

with a true flux at the center of cell. Coefficient  $b_k$  is the known fixed number. Eq. (3) provides new true flux into negative numerical viscosity term. It prevents minus numerical viscosity term around shock.

#### 3.3 Numerical schemes

Table 1 Numerical schemes tested in this paper

	Nonlinear Interpolation	Flux evaluation	Linear interpolation
MUSCL	3 <sup>rd</sup> -order MUSCL	AUSMDV	2 <sup>nd</sup> -order central-difference
W3M4	3 <sup>rd</sup> -order WCNS	AUSMDV	Eq.(1) with 4 <sup>th</sup> -order coefs
W5M6	5 <sup>th</sup> -order WCNS	AUSMDV	Eq.(1) with 6 <sup>th</sup> -order coefs
W7M8	7 <sup>th</sup> -order WCNS	AUSMDV	Eq.(1) with 8 <sup>th</sup> -order coefs
W3MN4	3 <sup>rd</sup> - order WCNS	AUSMDV	Eq.(2) with 4 <sup>th</sup> -order coefs
W5MN6	5 <sup>th</sup> - order WCNS	AUSMDV	Eq.(2) with 6 <sup>th</sup> -order coefs
W7MN8	7 <sup>th</sup> - order WCNS	AUSMDV	Eq.(2) with 8 <sup>th</sup> -order coefs

This paper validated the numerical schemes newly introduced into the flux calculation. The numerical schemes compared in this paper are shown in Table 1, where MUSCL is the scheme combined with MUSCL and AUSMDV. “WaMb” is the scheme combined WCNS with AUSMDV

and ordinary linear interpolation (Eq. (2)), where “a” is the order of WCNS and “b” is the order of linear interpolation. Similarly, “WaNb” is the scheme combined WCNS with AUSMDV and suggested linear interpolation Eq. (3)).

## 4 Code Validation

Unsteady term and convective term are validated by solving the Riemann problem using compressible Euler equations and comparing with its exact solution. This study utilized Sod problem<sup>[10]</sup>, where air is used as gas and its chemical reaction is inactive to compare with the exact solution. Moreover, to validate that shock is precisely captured for the experimental scale, the tube length is set to 2m. The left end of the tube is set to  $x=0$ .

### 4.1 Shock tube problem

This study calculates the performance of capturing shock front and contact discontinuity front. In this problem, the tube is separated by the left room at high pressure and the right room at low pressure and the wall between the rooms is removed at  $t=0$ . This problem is calculated under the condition that the specific heat ratio equals to 1.4, the grid point is 101 and CFL condition is 0.2. Air is used as gas.

Table 2 Initial conditions of Sod problem

	$\rho$ [kg/m <sup>3</sup> ]	$u$ [m/s]	$p$ [atm]
$x \leq 1.0$ m	9.39	0.0	10.0
$x > 1.0$ m	1.17	0.0	1.0

Fig.1 shows the result of comparison among several schemes of space derivative term. Fig. 1(b) is the enlarged view around the contact discontinuity. "Reference solution" in Fig.1 is the exact solution of Sod problem. All schemes obtain the value close to the quasi-exact solution to show that the coding of all schemes provides good calculation. In addition, Fig.1 shows that the higher the order of scheme is, the closer the value gets the quasi-exact solution.

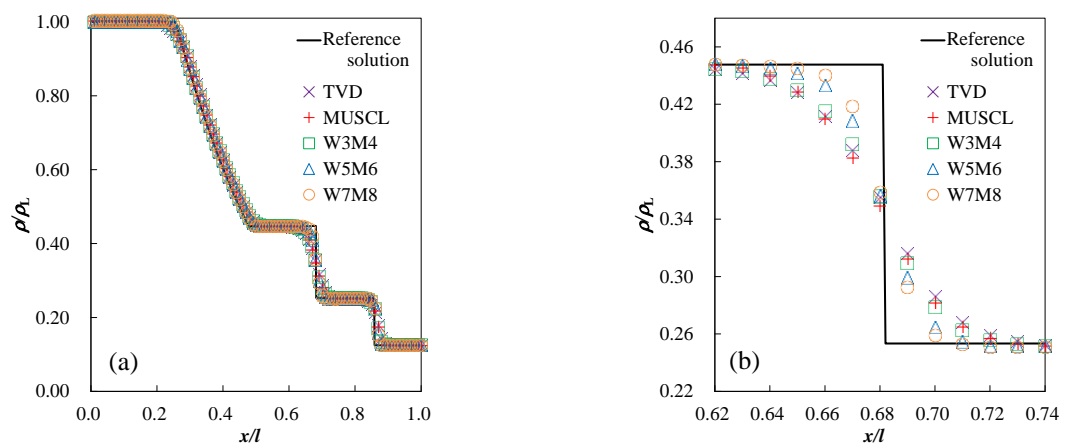


Fig.1 Density distribution of Sod problem computed by MUSCL, W3MN4, W5MN6, and W7MN8. Density  $\rho$  is nondimensionalized by the initial density  $\rho_L$ .

## 5 Two-dimensional simulation

The present paper uses double Mach reflection<sup>[13]</sup> (DMR) for two-dimensional validation. DMR calculation provides that the shock at Mach 10 comes to the area that has a 60 degrees ramp against the shock. The present paper simulates that the wall is set horizontally and the shock comes to the wall

obliquely. As the shock reflects at the wall, a jet of denser gas appears at the wall and a vortex occurs to the jet downstream. The equally intervalled orthogonal lattice points are used and the grid length is established as 4.167mm. The area shown is  $241 \times 961$  points and is established at the lower right corner of the calculation area. The initial condition is described below. “S” and “a” of lower subscript are the area behind and ahead of the shock. The specific heat ratio is 1.4. For the comparison, time step is set to  $0.2\mu\text{s}$  and CFL condition is set to 0.2. Air is used as gas.

$$U_s = (\rho[\text{kg/m}^3], u[\text{m/s}], v[\text{m/s}], p[\text{atm}])^T = (0.63, 2479.0, -1431.0, 1.19) \quad (5)$$

$$U_a = (\rho[\text{kg/m}^3], u[\text{m/s}], v[\text{m/s}], p[\text{atm}])^T = (0.12, 0.0, 0.0, 0.01) \quad (6)$$

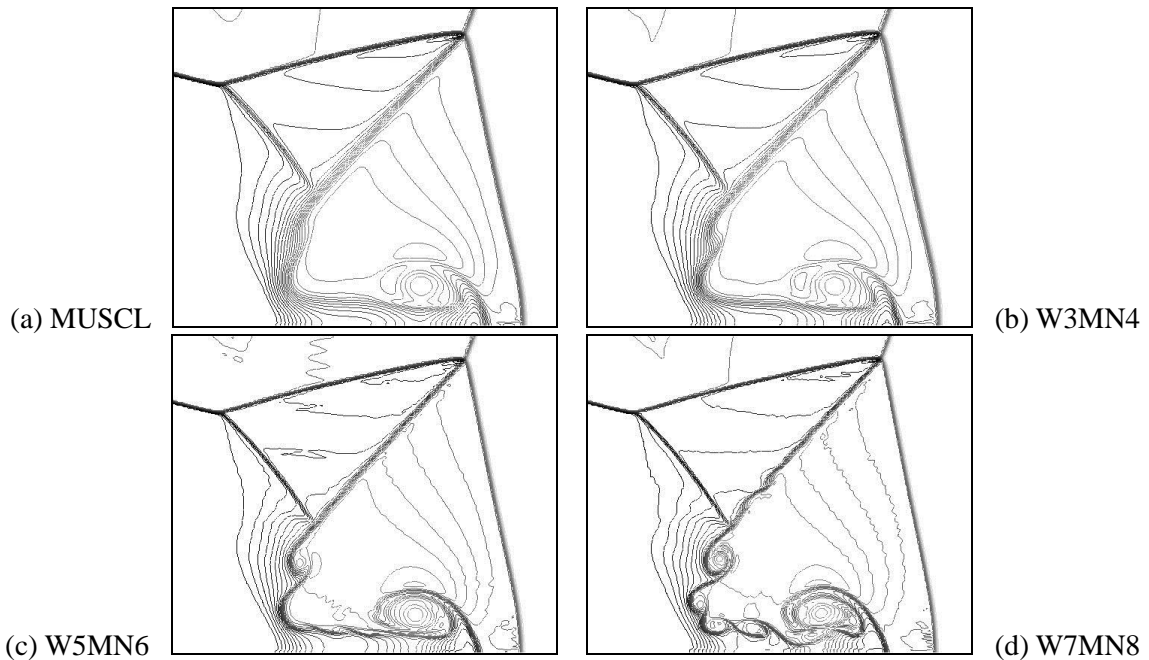


Fig. 2 The enlarged view of the density contour in the downstream computed by (a) MUSCL, (b)W3MN4, (c)W5MN6 and (d)W7MN8.

Fig. 2 indicates the result of DMR. Fig. 2(a-d) is the enlarged view around the vortex downstream. As the order of WCNS is high, the high resolution and the detail structure such as vortexes appear. The ratio of whole numerical time against MUSCL is W3MN4: 6.3, W5MN6: 9.3, W7MN8: 12.5.

## 6 Two-dimensional simulation of detonation

As an application, this study shows two-dimensional simulation of the detonation that propagates in the tube with a constant length channel.

### 6.1 Numerical conditions

For the computational area, the equally intervalled orthogonal lattice of points is used and the grid size is established as  $2.5\mu\text{m}$ . For the numerical condition,  $\text{H}_2/\text{Air}$  premixed gas is set at the equivalence ratio 1.0, initial pressure  $p_0$  1.0atm and initial temperature  $t_0$  300K. As for the boundary conditions, the mixture gas flows from the right side boundary of the calculation area at about 90% of the CJ velocity. The numerical result of one dimensional detonation is pasted in about 80% of the area from the left end. At this point, the one-dimensional detonation has already established there. To promote two-dimensional behavior, we set the disturbance behind the detonation front. In the left hand boundary, a rarefaction wave is pasted according to the method of Gamezo et al.<sup>[14]</sup> used for the purpose to maintain CJ velocity. The upper and lower side boundaries are adiabatic and slip wall.

## 6.2 Computational result and discussion of simulation

CFL condition that needs for each scheme is shown in Table 4, where the CFL condition of every scheme with Eq. (2) equals or is lower than 0.2. However, CFL condition of W3MN4 case and W5MN6 with Eq. (3) equals or is higher than 0.7 and these schemes are able to calculate the problem smoothly. On the other hand, CFL condition of W7MN8 is 0.3 and W7MN8 is not able to calculate the problem smoothly.

Fig. 3 shows the ratio of 1000 calculation time by WCNS method against the MUSCL case. Because of time step and  $x$  and  $y$  directions, when the grid length is doubled, numerical time increases eight times. If the resolution of W5MN6 is the same as that of MUSCL that is obtained on the doubled grid length, even after taking into consideration of the original time difference, MUSCL takes about four times more than W5MN6 to calculate the detonation with similar resolution. For the improvement of resolution, small grid size has also been applied to get a high resolution using AMR method. Due to such effect of grid size and time step, it is concerned that the approach by improving the scheme is less costly than that by the small grid size.

Table 4. Comparison with the CFL number of each scheme

	MUSCL	W3M4	W5M6	W7M8
CFL Condition	0.8	0.2	0.1	0.1
		W3MN4	W5MN6	W7MN8
CFL Condition		0.8	0.7	0.3

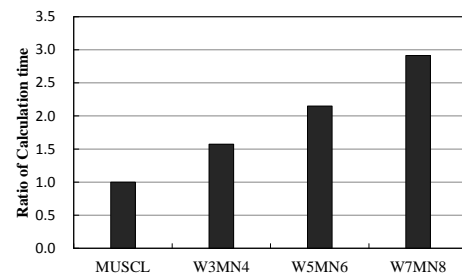
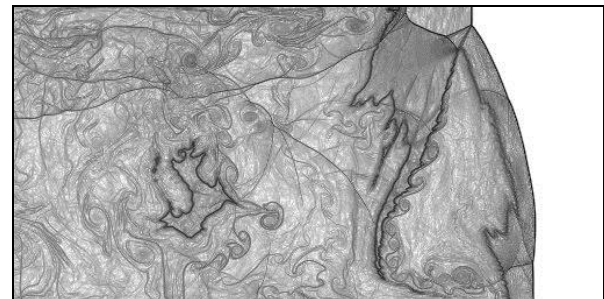
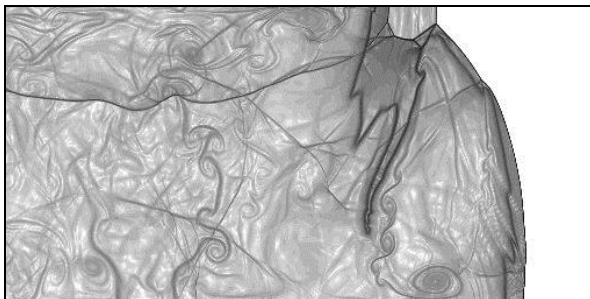
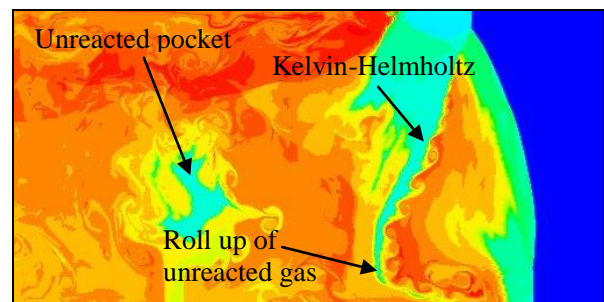
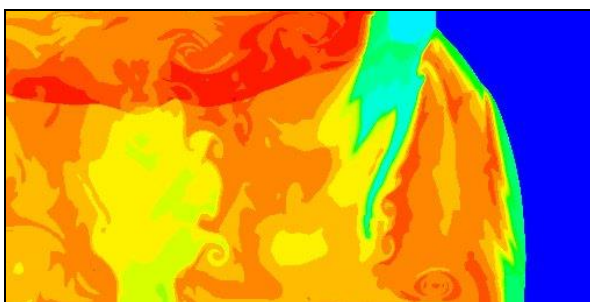


Fig.3. Ratio of 1000 calculation time



(1) Density gradient



(2) Temperature

(a) MUSCL ( $t=97.1\mu\text{s}$ )

(b) W5MN6 ( $t=116.1\mu\text{s}$ )

Fig. 5 Density gradient(1) and Temperature contours(2) for detonation in  $\text{H}_2/\text{Air}$  gas mixture computed by (a) MUSCL and (b)W5MN6

In the simulation with chemical reactions, a slight change of temperature and pressure changes the whole phenomena. Therefore, we compare the detonation fronts of two scheme cases when the

structure of detonation front is qualitatively similar. All schemes capture Mach stem, incident shock, reflection shock and transverse waves. Detailed structure of detonation front is shown in all schemes, but W5MN6 and W7MN8 clearly capture Kelvin-Helmholtz vortices at slip fronts.

Fig.5 shows density (1) gradient and (2) temperature profile of (a) MUSCL and (b) W5MN6 on the detonation front. According to Fig.5, W5MN6 captures the structure of the detonation front such as vortex further in detail. Moreover, in the area “Roll up of unreacted gas” in Fig.3(b), it is confirmed in detail that the unburned gas is rolled up. The unburnt gas rolled up moves the area of unburned gas at the downstream of transverse wave enlarged and it shows clearly unburned gas pocket. W5MN6 enables the progress of generating unburned gas pocket clearly.

## 7 Conclusion

In this paper, WCNS is introduced into the detonation code to analyze detonation in H<sub>2</sub>/air mixture. From one-dimensional simulation, it is confirmed that WCNS improves the resolution. The higher the order of WCNS is, the closer to the exact solution the value becomes. By results of Double Mach Reflection, it is confirmed that the higher order WCNS captures the two-dimensional structure of supersonic flows more clearly. From two-dimensional simulation of detonation, WCNS makes it possible to capture the detail structure and the detail process of the generation of detonation. Furthermore, the robustness of the linear interpolation improved by Nonomura and Fujii is confirmed and it is verified that detonation is able to be simulated smoothly and in detail with WCNS.

## References

- [1] Taki S, Fujiwara T. (1978). Numerical Analysis of Two-Dimensional Nonsteady Detonations, AIAA J.. 16: 73
- [2] Mazaheri K, Mahmoudi Y, Radulescu M I. (2012). Diffusion and hydrodynamic instabilities in gaseous detonations, J. Comb. and Flame. 159: 2138
- [3] Asahara A, Hayashi AK, Yamada E, Tsuboi N. (2012). Generation and Dynamics of Sub Transverse Wave of Cylindrical Detonation. Combust. Science, Tech. 184. 10: 1568
- [4] Wada Y, Liou M. (1994). A Flux Splitting Scheme with High Resolution and Robustness for Discontinuities, AIAA J.. 32: 94
- [5] Deng XG, Zhang H. (2000). Developing High-Order Weighted Compact Nonlinear Schemes, J. Comput. Phys. 165: 22
- [6] Zhang S, Jiang S, and Shu CW. (2008). Development of Nonlinear Weighted Compact Schemes with Increasingly Higher Order Accuracy, J. Comput. Phys. 227: 7294
- [7] Nonomura T, Iizuka N, and Fujii K. (2010). Freestream and Vortex Preservation Properties of High-Order WENO and WCNS on Curvilinear Grids, J. Comput. Fluid. 39: 197
- [8] Nonomura T, Fujii K. (2012). Robust Explicit Formulation of Weighted Compact Nonlinear Scheme, J. Comput. Fluids. printing.
- [9] Petersen EL, Hanson RK. (1999). Reduced Kinetic Mechanisms for Ram Accelerator Combustion, J. Propulsion and Power. 15: 591
- [10] Gottlib S, Shu CW. (1998). Total Variation Diminishing Runge-Kutta Schemes, J. Math. Comput. 67: 73
- [11] Van Leer B.(1977). Toward the Ultimate Conservative Difference Scheme. 4, A Ner Approach to Numerical Convection, J. Comput. Phys. 23: 276
- [12] Sod GA. (1978). A Suvey of Several Finite Difference Methods for Systems of Nonlinear Hyperbolic Conservation Laws, Comput. Phys. 27: 1
- [13] Woodward P, Collela P. (1984). The numerical simulation of two dimensional fluid flow with strong shocks, J. Comput. Phys. 54: 115
- [14] Gamezo VN, Desbordes D, Oran ES. (1999). Two-Dimensional Reactive Flow Dynamics in Cellular Detonation Waves, Shock Waves. 9:11